DOI: 10.1021/ma101390j

Macromolecules
ARTICLE

Investigation of Polymerization Mechanisms of Poly(*n*-Butyl Acrylate)s Generated in Different Solvents by LC−ESI−MS^2

Junkan Song,[†] Jan W. van Velde,[†] Luc L. T. Vertommen,[†] Leo G. J. van der Ven,[‡] Ron M. A. Heeren,[§] and Oscar F. van den Brink*,[†]

[†]*Research, Development and Innovation, AkzoNobel, Deventer, The Netherlands,* [‡]*Car Refinishes, AkzoNobel, Sassenheim, The Netherlands, and* [§]*FOM Institute for Atomic and Molecular Physics, Amsterdam, The Netherlands*

Received June 22, 2010; Revised Manuscript Received July 30, 2010

ABSTRACT: Liquid chromatography-electrospray ionization-tandem mass spectrometry (LC−ESI−MS^2) was employed for the characterization of three poly(*n*-butyl acrylate)s. These polymers were produced at high temperature using the same initiator, *tert*-butyl peroxy-3,5,5-trimethylhexanoate, but in different solvents, viz. pentyl propionate, xylene and butyl acetate. Exact mass experiments performed on these polymers in an Orbitrap instrument supplied valuable information on the end group structures. Study of the data allowed identification of many reactions during the polymerization such as beta-scission and chain transfer to solvent or radical transfer to solvent from the initiator. Different fragmentation pathways were observed from the same precursor mass on MS/MS experiments, indicating the presence of isomers. The comprehensive assignment of the peaks in the LC−MS data allowed us to describe the end group distribution in a semiquantitative way. The results clearly show that the relatively reactive solvents used for polymerization have strong influences on the polymer composition.

Introduction

Acrylic polymers serve a huge global market. Noted for their transparency and resistance to breakage, they have been widely used in coatings, in medical and recently also in pharmaceutical areas.[1−3] Radical polymerization using peroxide initiators offers control of molecular weight and dispersity.[4] Recent developments on controlled/living radical polymerizations, such as ATRP, offer much better control of these variables.[5] However, only very limited number of commercially available products are produced in such way. Radical polymerization is still used as a major industrial method to produce acrylic polymers.

The mechanism of radical polymerization has been well-studied for many years. Three stages are involved in the polymerization: initiation, chain propagation and chain termination. Scheme 1 shows the possible initiation species by the peroxide initiator (Trigonox 42S) which was used in this study. The many possibilities of initiation species will result in different end groups.[6] An octyl radical (C_8H_{17}•, r) is the major initiation species for this peroxide under the conditions used here. The other part of the initiator, the butyloxyl radical, can undergo several possible reaction routes. One is to produce acetone and methyl radicals (CH_3•, m) that also start initiation. A second initiation route is to react with the solvent used in the polymerization and transfer the radical to the solvent; the solvent radical formed will then start the polymerization. Another possible initiation route is to transfer the radical to monomer.

Radical polymerization of alkyl acrylate at relatively high temperature introduces some specific initiation and termination mechanisms. An intramolecular chain transfer reaction, namely intramolecular backbiting, observed in many cases,[7−10] will increase the complexity of the end group distribution. The backbiting reaction forms a tertiary carbon-centered radical by hydrogen abstraction to a secondary carbon at the chain end or a tertiary carbon on the main chain. The carbon-centered radical formed undergoes β-scission to generate a β-scission radical and a terminally unsaturated chain. This mechanism is shown in Scheme 2. The chain that undergoes β-scission will therefore generate four oligomers through four pathways, namely β1a, β1b, β2a and β2b, which can be terminated in many different ways. The chain from pathway β1a is identical to the normal radical propagation species and could be terminated by hydrogen abstraction, combination or disproportionation. The other end of the chain, X as shown in Scheme 2, could be from the initiator radical or the solvent radical. Pathway β1b will generate a chain terminated by an unsaturated end group formed by β-scission at one side of the chain. Similarly, β2a will also form a terminally unsaturated chain but with the other side of chain with end group formed by either the initiator radical or the solvent radical. The last oligomer formed by β-scission pathway β2b can be terminated by hydrogen abstraction, as well as by combination or disproportionation. As stated in Scheme 2, these four routes will all form different end groups and result in different masses. The unique mass features are so distinctive that MS is a very suitable tool to recognize them. However, when the secondary carbon on the main chain is terminated by branching to form a 3-arm or a 4-arm star, the products formed in this pathway have identical mass to the linear structure and therefore cannot be distinguished by MS. Information on branching level could be obtained by ^{13}C NMR spectroscopy.[11] Furthermore, all the oligomer formed by β-scission could undergo further backbiting, β-scission or branching. The possibility however is very low in the low molecular weight fraction of the polymer. There is also evidence that chain transfer may not occur to the backbone but to the side chains.[12]

In addition, chain transfer to solvent is also reported as a common reaction in radical polymerization. The solvent effect was observed and investigated in several previous studies.[13−15]

*Address correspondence to O.F.v.d.B. at AkzoNobel, Research, Development and Innovation, P.O. Box 10, Deventer, 7400 AA, The Netherlands. E-mail: oscar.vandenbrink@akzonobel.com.

 Published on Web 08/11/2010

Scheme 3 shows the reactions of chain transfer to solvent in the cases investigated in this study. The solvent radicals shown in the scheme are the most likely structures formed under these conditions.

Understanding the structure and quantity of the end groups is important information to have for polymer structure design and to control the physical or chemical properties. A great variety of techniques has been developed to determine the structural properties of polymers since their invention. The conventional technique to obtain the molecular weight and dispersity of polymers is gel-permeation chromatography (GPC);[16] Fourier-transform infrared (FTIR) spectroscopy and nuclear magnetic resonance spectroscopy (NMR) spectroscopy[17] are used to give structural information, while differential scanning calorimetry (DSC)[18] is used to determine the crystalline structure of polymers.

Over the past decades, the development of "soft" ionization methods such as electrospray ionization (ESI) and matrix-assisted laser desorption/ionization (MALDI)[19−28] allowed mass spectrometry to become an important tool for the characterization of synthetic polymers. Characterization of synthetic polymers of relatively high molecular weight can be achieved due to the formation of multiply charged ions generated by electrospray ionization.[29] Information such as average molecular weight (in some cases) and polymer structures may be obtained.[30−33]

Furthermore, tandem mass spectrometry (MS/MS) has been employed to many synthetic polymer systems for structural studies. The very first MS/MS studies used magnetic sector instrumentation and date back to 1985.[34,35] Many instruments for multistage mass spectrometry have been developed which perform MS/MS. Tandem MS/MS studies on synthetic polymers are commonly performed on tandem quadrupole-time-of-flight[36−38] and ion trap[39−43] mass spectrometers. Collision-induced dissociation (CID)[36,44] is the method used in most cases to fragment the selected precursor ions. The precursor ions are accelerated by electrical potential to high kinetic energy in the vacuum and then collide with neutral gas atoms. Part of the kinetic energy is converted into internal energy in the collision. This results in bond breakage and the fragmentation of the precursor ions. The fragment ions produced are used for partial or complete structural determination.

Junkers et al.[11] demonstrated using ESI−MS for detailed mapping of the product spectrum in acrylate polymerization in order to obtain mechanistic information. In addition, research was performed on acrylic polymers synthesized by free radical polymerization in the presence of chain transfer agent which used ESI−MS for quantification.[45] In this study, we went a step further to characterize three poly(*n*-butyl acrylate)s (PBAs) synthesized by free radical polymerization using high resolution and high accuracy LC−ESI−MS^n. The PBAs were polymerized under high temperatures but in different solvents. The combined mass of the end groups of a polymer may be calculated from the high accuracy and resolution mass spectrometric data. MS^n spectra show different fragmentation patterns for the same nominal mass and thus allow discrimination between isomers deriving from different end groups. We utilized these different fragmentation patterns in an attempt to aid quantification of the different initiation and termination reactions during free radical polymerization of PBA in the relatively lower molecular weight region of the spectra.

Scheme 1. Initiation mechanism for Trigonox 42S initiator

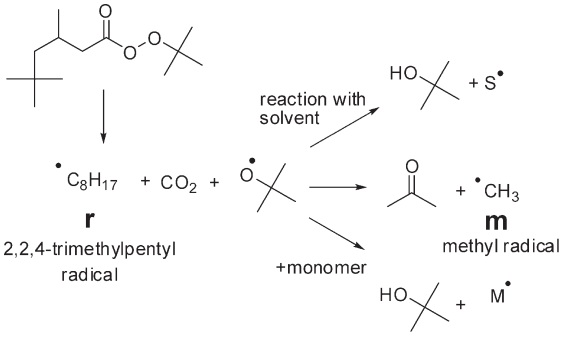

Scheme 3. Chain Transfer to Solvent in the Cases of Pentyl Propionate, Xylene, and Butyl Acetate (P• = Propagating Chain)

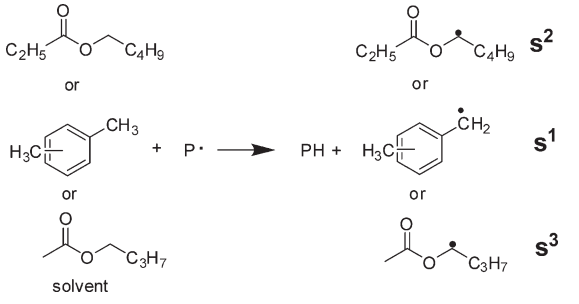

Scheme 2. β-scission of alkyl acrylate radical polymerization at relatively high temperature

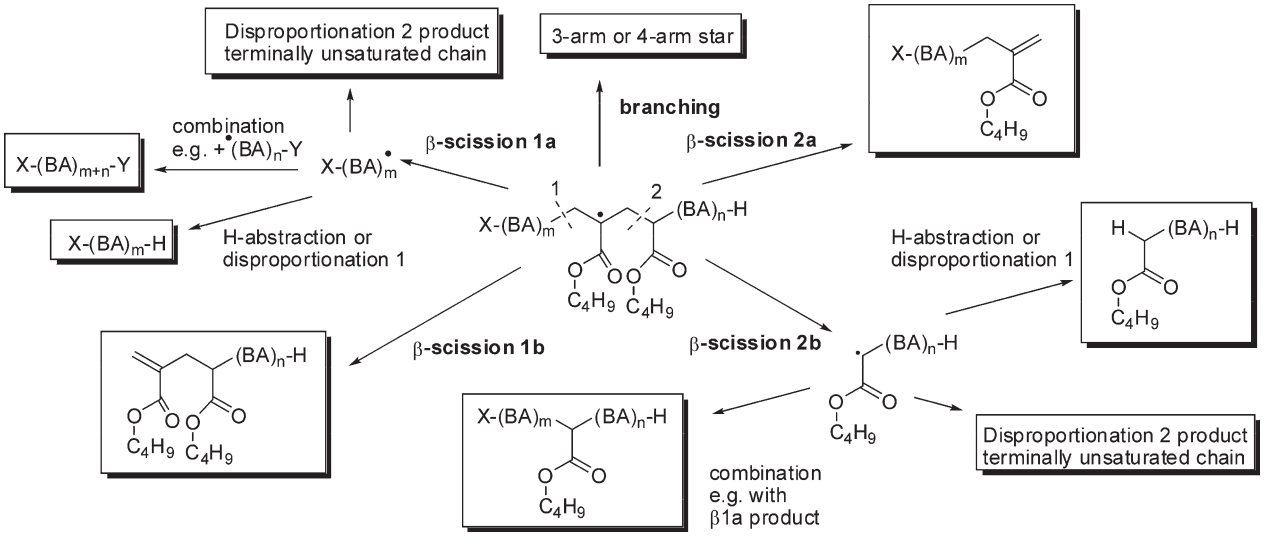

Table 1. Polymerization Information of the Three PBAs[a]

sample code	A	B	C
solvent	pentyl propionate	xylene	butyl acetate
M_n (g/mol)	2467	2800	3761
M_w (g/mol)	4757	5510	10 186
polymerization temperature (°C)	168	140	140

[a] Monomer used was butyl acrylate in all samples. Initiator used was *tert*-butyl peroxy-3,5,5-trimethylhexanoate (Trigonox 42S).

Experimental Section

Polymer Synthesis. All PBA samples were obtained from AkzoNobel Car Refinishes, Sassenheim, The Netherlands. They were prepared by radical polymerization using the same initiator, *tert*-butyl peroxy-3,5,5-trimethylhexanoate, but different temperatures and solvents, viz. pentylpropionate (A), xylene (B), and butyl acetate (C). The molecular weight averages of the resultant PBA samples were measured by GPC calibrated with polystyrene standards. Table 1 lists the composition, the process and the results obtained by GPC characterization of the samples.

Mass Spectrometry. Mass spectra were acquired by liquid chromatography-ESI−MS (LC−ESI−MS). A Thermo Scientific LTQ Orbitrap XL mass spectrometer was used in this study. The LC system was an Agilent 1100 series LC binary pump with DAD detector. The LC column in the LC−ESI−MS setup was an Alltech Kromasil C18 (150 mm × 4.6 mm). During analysis, the column temperature was thermostatized at 30 °C. A gradient of tetrahydrofuran (THF) (Sigma-Aldrich)/H_2O (from Millipore Direct-Q) was used as mobile phase. Formic acid (FA) (Fluka) at a level of 0.1% was added to both mobile phases. Samples with a concentration of 2 mg/mL in methanol were prepared. Data were processed and analyzed using Thermo Scientific Xcalibur 2.0 data systems.

Results and Discussion

LC separation was used prior to and online with MS. A wide range of gradients was tested to optimize the LC separation. The best separation of the PBA samples was achieved using gradient from 50% THF/50% H_2O to 100% THF in 30 min. All oligomers were ionized by sodium ions, forming $[M + Na]^+$ species, presumably from residual sodium salts in the solvents. Figure 1 shows the summation mass spectra (1−18 min) of all three PBA samples from the ESI−Orbitrap LC−MS experiments. The combination of LC separation and summation over the separated peaks serves the purpose of mitigating or decreasing the effects of ion suppression that may occur when infusion analysis is used. On the basis of the GPC data mentioned previously, the mass spectral data is only from a low molecular weight fraction of the full distribution. Several series of peaks start at m/z 513 continuing to greater than m/z 1448 with a separation of 128 Da between each group (the acquisition range of the MS was m/z 500 to 1500). The 128 Da separation between peaks is, clearly, attributed to the mass of BA, of which the molecular formula is $C_7H_{12}O_2$ and the theoretical exact mass is 128.0837 Da. Multiply charged peaks were observed with very low intensity and therefore not taken into consideration here. The summed LC−MS spectrum alone, however, was not sufficient to identify the different structures in the complicated product systems.

The many possible initiation and termination mechanisms yield a great number of potential combinations. In the spectra of all three PBA samples, one of the most intense and common set of peaks are those from series β^{2b}, m/z 523 + (n − 3) × 128, irrespective of the solvent used in polymerization. The mass-to-charge ratios of eight peaks from this series in all three PBAs were plotted against the number of BA units, as shown in Figure 2 (only for PBA(C)).[46] The residual masses were 139.0731 Da for PBA(A), 139.0734 Da for PBA(B) and 139.0733 Da for PBA(C), as calculated using linear regression. The monomer masses calculated were 128.0834 (Δ = 2.34 ppm) for all three PBAs and the standard deviations were 0.56 ppm (A), 0.57 ppm (B) and 0.39 ppm (C). The chemical composition of the combined mass of the end groups is $[C_6H_{12}O_2]Na^+$. (Δ = 0.72 ppm (A), 2.88 ppm (B) and 2.16 ppm (C)). It agrees well with the end group structure formed by an initiating β-scission radical (pathway β2b) and terminated by hydrogen abstraction or disproportionation. The structure of the chains in this series is shown in Scheme 4

Another very intense series of peaks in all three spectra is series β^{1b}, m/z 535 + (n − 3) × 128. The same identification process as used for series β^{2b} was applied for this series. A residual mass of 151.0724 Da was calculated using linear regression for all three PBAs. The elemental composition of this mass is proposed to be $[C_7H_{12}O_2]Na^+$ (Δ = 4.0 ppm). The end group structure attributed to this series is the result of β1b, β-scission forming an unsaturated chain end. The proposed structure is given in Scheme 4. In this case, the errors of the experimental and theoretical BA mass are 0.78 ppm for PBA(A), PBA(B) and 1.56 ppm for PBA(C). The standard deviations are 0.34 ppm (A), 0.59 ppm (B), and 0.46 ppm (C).

Using this identification process, another end group combination was identified in all three PBAs resulting from (1) the radical initiator and terminated by either hydrogen abstraction or disproportionation and (2) β-scission pathway β1a and then terminated by either hydrogen abstraction or disproportionation. The two different pathways were indistinguishable because they result in identical elemental composition and structure. The series r, showing peaks at m/z 521 + (n − 3) × 128 was found to have a residual mass of 137.1303 Da from PBA(A), 137.1297 Da from PBA(B), and 137.1303 Da from PBA(C). This mass is attributed to the combined end groups having elemental composition $[C_8H_{18}]Na^+$ (Δ = 1.46 ppm for PBA(A) and PBA(C), 2.92 ppm for PBA(B)). It indicates that the chain has an octyl end group from the peroxide initiator, formed as described in Scheme 1, and a hydrogen at the other end. The differences between the experimental and theoretical BA mass within the series are 1.56 ppm (A) and 0.78 ppm (B and C). The standard deviations were 0.25 ppm (A), 0.27 ppm (B), and 0.24 ppm (C). In a similar way, series m, m/z 551 + (n − 4) × 128 with residual mass of 39.0211 Da from PBA(A), 39.0200 Da from PBA(B), and 39.0211 Da from PBA(C) was found to have $[CH_4]Na^+$ as end group composition (Δ = 15.4 ppm (for A and C), 12.8 ppm (for B)). The molecules in this series are proposed to originate from initiation by a methyl radical from the peroxide initiator and termination by hydrogen abstraction or disproportionation; or from a methyl radical initiated chain undergoing β1a followed by termination through hydrogen abstraction or disproportionation (see Scheme 1 for the mechanism of methyl radical formation from the initiator). The differences between the experimental and theoretical BA mass are 0.78 ppm (A), 0.51 ppm (B), and 2.34 ppm (C). The standard deviations were 0.22 ppm (A), 0.34 ppm (B), and 0.41 ppm (C).

Two more series that are observed in all three PBA spectra are β^{2a}r and β^{2a}m. Both of the series result from β-scission pathway β2a, forming an unsaturated end group. The difference between the two is that series β^{2a}r was octyl radical initiated and series β^{2a}m was methyl radical initiated. Both the octyl radical and the methyl radical were formed from the peroxide initiator (see Scheme 1). A comparison of the experimental data with the theoretical data for selected oligomers from PBA(C) is presented in the Supporting Information.

There is a unique series, s[1], m/z 513 + (n − 3) × 128, that is only observed in the spectrum of PBA(B), where xylene was used as the solvent. The residual mass calculated using linear regression is 129.0678 Da. The elemental composition of the residual mass is

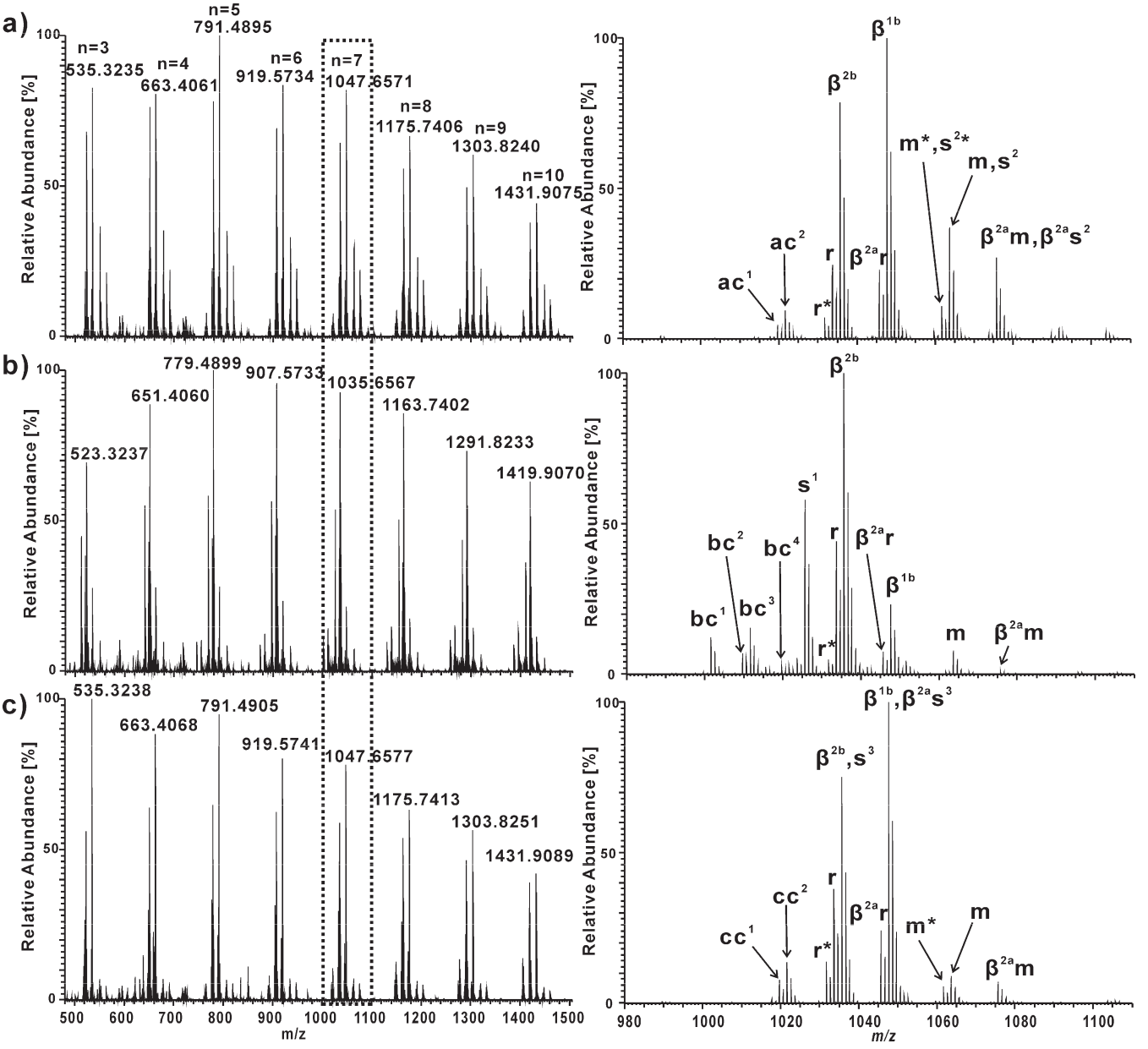

Figure 1. Left: Summation mass spectra (1′-18′) of all three PBA samples on LC/ESI−Orbitrap MS. Right: Expanded spectra (m/z 980−1110) of the corresponding samples. The solvents used in the polymerization were (a) pentylpropionate, (b) xylene, and (c) butyl acetate.

$[C_8H_{10}]Na^+$ (Δ = 2.32 ppm). It is assigned as arising from chain transfer to solvent or radical transfer from initiator to solvent. A xylol radical is formed when a growing polymer chain abstracts hydrogen from a methyl group in the xylene solvent (Scheme 3). As mentioned in the introduction, another mechanism for the formation of a xylol radical could be the abstraction of a hydrogen by an initiator radical. The structural formula of the ion noted from the data is $[C_8H_9\text{-}(BA)_n\text{-}H]Na^+$. The difference between the experimental and theoretical BA mass is 1.56 ppm and the standard deviation of the experimental mass is 0.52 ppm.

Since all three PBA samples were polymerized under similar conditions, it is expected that chain transfer to solvent or solvent radical initiation has taken place in each of the polymerizations, especially as the solvents used here are prone to this phenomenon. Calculation of the masses of PBA oligomers with end groups resulting from solvent radical formation by initiator radical transfer to solvent or chain transfer to solvent, and then terminated by either hydrogen abstraction or disproportionation indicated that they would overlap with series m and series β^{2b}, in PBA(A) (from pentyl propionate) and PBA(C) (from butyl acetate) respectively, as they have the same elemental composition.

LC coupled with multistage mass spectrometry, when set up properly, can discriminate between isomers with exact same mass by producing different fragments. Therefore, LC−MS^2 experiments were performed to obtain fragmentation information and thus investigate the presence of structural isomers with different end group structures.

Figure 3 shows the LC traces (extracted ion count chromatogram, EIC) of m/z 935.61 for PBA(A) (polymerized in pentyl propionate) and PBA(B) (polymerized in xylene). Automatic MS^2 was engaged throughout the whole separation. This procedure performs MS/MS of every base peak in the individual MS spectra throughout the entire LC experiment. Only one LC elution peak was observed for PBA(B). Figure 4 shows the partial LC−MS^2 spectra of m/z 935.6100 (PBA(A) and PBA(B)) obtained in the Orbitrap instrument. A single fragmentation pathway was observed producing a peak at m/z 879.54 in the

$LC-MS^2$ spectrum of PBA(B). The pathway involves a loss of m/z 56 (C_4H_8) from the side chain of the PBA, indicating that no backbone cleavage happened during the fragmentation process. But from the chromatogram of PBA(A), two LC peaks were observed at 13.2 and 14.0 min. A loss of m/z 74 in addition to the m/z 56 loss was observed in the combined spectra summed across the whole LC chromatogram. Judging from the corresponding elution time, we propose this additional loss is from the polymer eluting at 13.2 min. The elemental composition of m/z 74 could either be $C_4H_{10}O$ or $C_3H_6O_2$. The LC−MS/MS data from the Orbitrap analysis showed that the accurate mass of this loss is m/z 74.0391 which agrees well with the exact mass of $C_3H_6O_2$ (m/z 74.0368) rather than $C_4H_{10}O$ (m/z 74.0732). In the spectra of PBA(A), the two different fragmentation pathways as well as the two LC peaks in the EIC of m/z 935.6100 prove that two isomers exist at this identical exact mass. Series s^2, which exclusively displays the loss of m/z 74, therefore results from chain transfer to the pentyl propionate solvent (or the pathway β1a). In this case, the molecular formula for m/z 935.6100 is $[C_8H_{15}O_2-(BA)_3-H]Na^+$. Scheme 5 plots the proposed fragmentation pathway, involving the loss of propanoic acid from the end of the polymer chain (from the initiation of the chain by the radical originating from the pentyl propionate solvent) that gives rise to the peak at m/z 861.5658. The same fragmentation pathway was observed in the spectra from Series $\beta^{2a}s^2$ resulting from β-scission pathway β2a.

Two similar cases, series s^3 and $\beta^{2a}s^3$, were identified as overlapping with series β^{2b} and series β^{1b} respectively in PBA(C) using LC−MS/MS. In both series (s^3 and $\beta^{2a}s^3$) a loss of m/z 60 (acetic acid) from the end of the polymer chain (resulting from the initiation by the butyl acetate solvent radical) was observed in MS/MS in addition to the m/z 56 side chain loss. The fragmentation mechanism is analogous to the one described in Scheme 5. The difference between series s^3 and series $\beta^{2a}s^3$ is that the former resulted from pathway β1a (or chain transfer to solvent) and the latter from the pathway β2a. An alternative to the high mass resolution approach described in this paper would be the use of

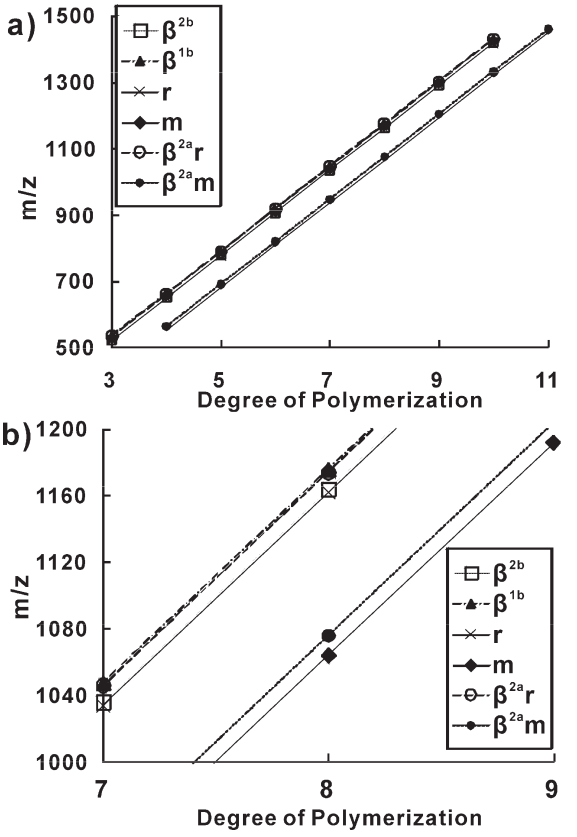

Figure 2. (a) Linear regression of m/z peaks of several series from PBA(C) (m/z 500−1500, degree of polymerization 3−11). (b) Expanded area of part a (m/z 1000−1200, degree of polymerization 7−9).

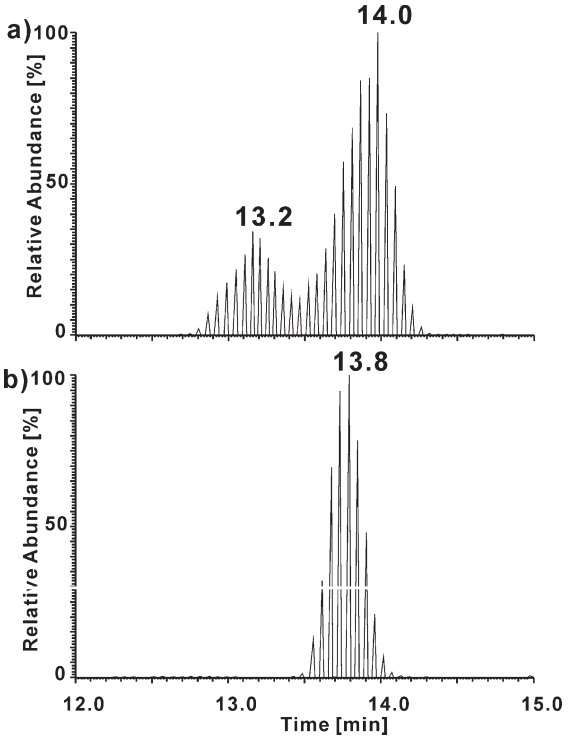

Figure 3. Partial (12′ − 15′) EIC traces for m/z 935.6 for (a) PBA(A) (polymerized in pentyl propionate) and (b) PBA(B) (polymerized in xylene) on LC−Orbitrap MS.

Scheme 4. Proposed Structures of the End Group Combination Series in Polymers PBA(A−C)

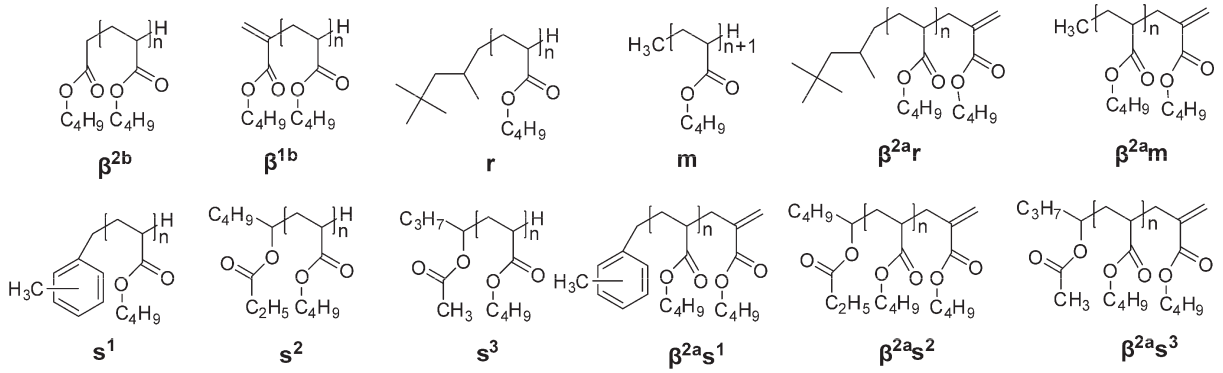

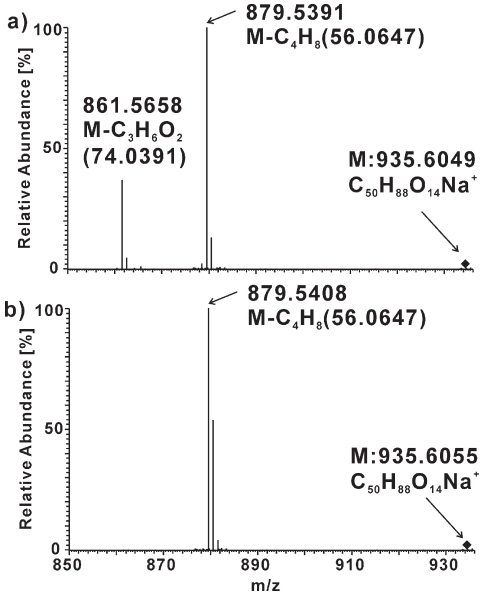

Figure 4. Partial LC − MS^2 spectrum of (a) m/z 935.6049 (PBA(A)) and (b) 935.6055 (PBA(B)) obtained on Orbitrap instrument.

Scheme 5. Proposed fragmentation of $[C_8H_{15}O_2{-}(BA)_6{-}H + Na]^+$ (m/z 935) from PBA(A)

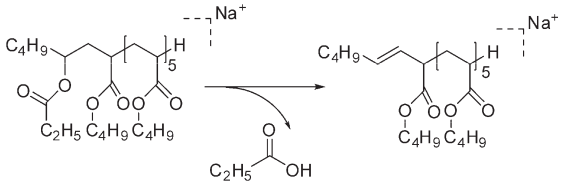

ion mobility spectroscopy (IMS)/MS to separate the different structural isomers in the gas phase.[47,48] This could also help differentiate between linear and branched oligomers of PBA.

Unsaturated terminated species formed by disproportionation were observed in the spectra of all three PBAs with relatively low intensities. For example, for series r*, m/z 519 + (n − 3) × 128, the residual mass calculated is 135.1138. Hence, the elemental composition is $[C_8H_{16}]Na^+$ (Δ = 4.44 ppm). The difference between the experimental and theoretical BA mass is 1.56 ppm and the standard deviation is 0.35 ppm. The disproportionation termination resulted in an unsaturated end group at one side of the polymer while the original initiation species sit on the other side. In the spectra, we could easily notice the mass difference of m/z 2.0157 (two hydrogens) with respect to the normal terminated chain. This mass difference is consistent for series r and r* (The average error is 0.7 mDa and the standard deviation is 0.5 mDa). Similar cases found in the spectra were, for example, series m* and β^{2a}r*.

The high accuracy and resolution data from the Orbitrap instrument also allow us to observe some less intense series of peaks that have m/z very close to the more intense series of peaks already discussed, which normally cannot be discriminated using mass spectrometers with relatively low accuracy and resolution (such as standard ion trap instruments). Figure 5 shows two peaks with 0.072 Da difference in PBA(B), generally pointing at exchange of O_2 against C_2H_8 in elemental composition. The second peak with a mass of m/z 777.5478 is from series r (Δ = 1.29 ppm). Through calculation, the elemental composition of the ion at m/z 777.4759 is assigned to $C_{41}H_{70}O_{12}$ (Δ = 0.03 ppm). The structure of this oligomer is proposed to result from the β-scission pathway β2b combined with termination by disproportionation. The resulting structure is shown in Figure 5. The series

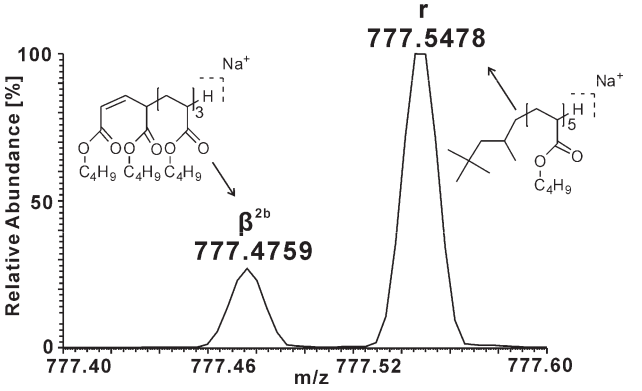

Figure 5. Expanded Orbitrap MS summation spectrum for PBA(B) (777.4000−777.6000).

is labeled as β^{2b}*. This lower intensity peak would not be observed with low resolution mass spectrometry since the peak would merge with the very intense neighboring peak. The high accuracy and resolution mass spectrometry allowed its detection.

Similarly, another series with low abundance was located in PBA(B), labeled as series $\beta^{2a}s^1$. We propose it to result from xylol radical initiated chain and terminated by β-scission pathway β2a. The theoretical combined end group mass of the series is m/z 141.0675 which is isobaric with the second isotopic peak (with two ^{13}C atoms) of series β^{2b} (141.0797). Unfortunately, only the first two peaks (trimer and tetramer) in the series were resolved. The peak observed at m/z 781.4913 in the spectra, where the pentamer would be expected, has a broader peak shape and does not allow the identification of the pentamer from series $\beta^{2a}s^1$. The required resolution at the pentamer (m/z 781.4861 $\beta^{2a}s^1$ and m/z 781.4983 β^{2b}) to distinguish these two peaks would be 64 000, which would require an instrument with even higher resolving power than the Orbitrap, such as FT-ICR MS. Moreover, the intensity of the second isotopic peak is also higher than in the normal isotope pattern from series β^{2b} in PBA(A) and PBA(C).

Evidence of the polymer chain terminated by combination was observed in the relatively low molecular weight region only at very low intensity. However, the intensity of the peaks of the same series increases when the degree of polymerization increases in all three PBAs. It is expected that termination by combination has a higher possibility to generate a longer chain rather than a short oligomer. In the expanded spectra of Figure 1, the peaks labeled with ac^1 and ac^2 in PBA(A), bc^1−bc^4 in PBA(B) and cc^1 and cc^2 in PBA(C) are all terminated by combination. As shown in Scheme 2, two types of combinations could happen in this polymerization system: (1) two chains both undergoing β1a and/or from standard initiation or chain transfer from solvent (as the structure is the same for these two species) and(2) one chain undergoing β1a and/or standard initiated or chain transfer to solvent initiated chain and the other undergoing β2b. Moreover, the resulting products from combination may have a large variety of combined end groups from the two initiator radicals and the solvent radicals. However, not every combination was observed in the spectra. For example, in the case of PBA(B), peaks in series bc^1 and bc^2 were formed by the combination of two chains both undergoing β1a and/or from standard initiation or chain transfer from solvent (bc^1, xylol end group at both ends; bc^2, xylol end group at one end and octyl end group at the other). Those in series bc^3 and bc^4 were formed by the combination of one chain undergoing β1a and/or from standard initiation or chain transfer from solvent and the other undergoing β2b (bc^4, xylol end group at both ends; bc^4, xylol end group at one end and octyl end group at the other). In PBA(A) and PBA(C), some of these combinations resulted in peaks that have mass-to-charge

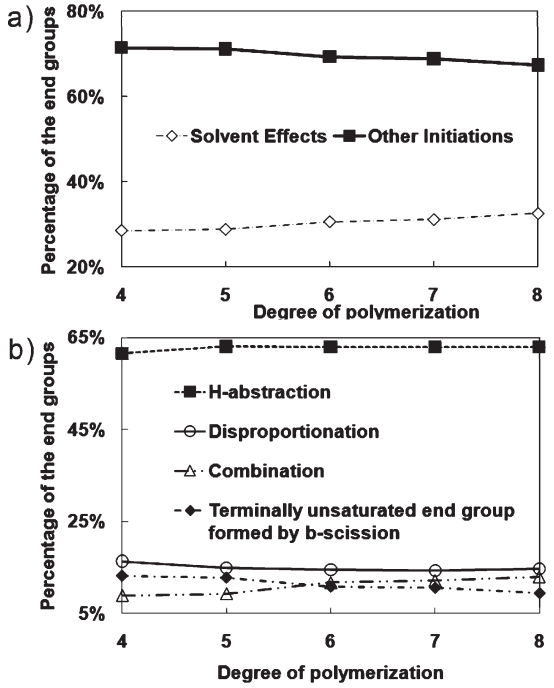

Figure 6. Comparison of the percentages (relative intensity) of PBA(B) with end groups formed from different (a) initiation and (b) termination mechanisms. Data derived from summing the respective peak intensities in LC−ESI−Orbitrap data.

ratios too close to the most intense peaks and hence not all of them are resolved. No combination with methyl or butyloxyl end-capped chains was observed in the spectra of any of the three PBAs.

Scheme 4 shows the proposed structures (without the cation adduct) for all major peak series identified in the ESI−MS spectra of PBA(A), PBA(B), and PBA(C). The corresponding series from disproportionation or combination are not presented. A table listing the combinations of initiation and termination mechanisms of these series and their corresponding combined end group masses is presented in the Supporting Information. Butyloxyl radical initiated chains were not observed in the spectra. This is attributed to this radical mainly contributing to the formation of methyl radicals and/or to radical transfer to solvent. The radical itself is also not large enough[6] to undergo a 1,5-H-shift reaction and then start an intramolecular chain-transfer reaction.

ESI−MS is not a fully quantitative method. It can still be used in a semiquantitative way to address the amount of polymer initiated or terminated by different mechanisms, especially at higher degrees of polymerization[45] (this is because any differences in end group structures should play a smaller role in the ionization mechanism, presuming that the cation used binds with the oxygens in the ester of the main chain predominantly, as may be indicated by previous results from other acrylic polymers[49]). The graph in Figure 6 was derived from the LC−ESI−MS data by summation of the peak intensities of the respective end group combinations in PBA(B) (from xylene). Series $\beta^{2a}s^{1}$ was not taken into consideration because the oligomers in this series that are larger than the tetramer could not be resolved from the second isotopic peaks in series β^{2b}. Detailed data and calculation can be found in the Supporting Information. As we suggested earlier, the data generally shows an increasing amount of end groups formed by combination of chains when the degree of polymerization increases. In the case of the radical polymerization of PBA in xylene, these data indicate that more than 30% of the chains were formed by the influence of solvent, either from initiator radical transfer to xylene or chain transfer to xylene. Hydrogen-abstraction is the main termination contributing 60% to the end group formed. Disproportionation is less frequently observed than hydrogen-abstraction and only contributes a modest 15% to the polymerization. Combination contributed 9% to the end group in the case of tetramer and the influence increased to 13% in octamer. The amount of chains with terminally unsaturated end group formed by two different β-scission pathways β1b and β2a is 13% for tetramer and decreases with the degree of polymerization, dropping to 9% for octamer. In the cases of PBA(A) and PBA(C), the existence of isomers originating from different initiation and termination mechanisms makes the quantitative study rather difficult to perform. The results here are in line with the previous study by Koo et al.[45] which showed that in the presence of chain transfer agents the proportions of β-scission products would be limited.

The β-scission reaction is theoretically not favored to happen to one specific side.[11] Therefore, the ratio of the products generated through β1b and β2a should be 1:1. However, it is difficult to calculate from the data we have since the intensity of peaks in series $\beta^{2a}s^{1}$ cannot be taken in consideration. The peaks in this series are not resolved as mentioned previously. Without the data from series $\beta^{2a}s^{1}$ (peaks in the series were generated from β2a), pathway β1b shows a relatively higher influence than β2a. The cause of this proposed difference in abundance is unclear, from the proposed mechanism (Scheme 2).

Conclusions

LC−ESI MS^2 of the three PBA samples identified many initiation and termination reactions during the polymerization, including peroxide initiator initiation, solvent radical initiation or chain transfer to solvent, four different β-scission pathways, H-abstraction, disproportionation and combination. The combination of these mechanisms generated a great variety of end groups for these polymers which were all identified by using high resolution LC−MS, although some of the series were not resolved at higher degrees of polymerization. Multistage MS showed different fragmentations for peaks that had identical exact mass but different elution times. Isomers were observed that originated from different initiation mechanisms. The high accuracy and resolution MS spectra obtained using the Orbitrap allowed discrimination of two isobars with 0.072 Da mass difference which could easily be overlooked in normal low mass accuracy and resolution MS. The comprehensive attribution of the peaks in the LC−MS data allowed us to address the end group distribution in a semiquantitative way for one of the polymers studied. Although the data do not allow semiquantitative comparison of the various initiation and termination mechanisms in all three PBAs, the results clearly show that the relatively reactive solvents used for polymerization strongly influence the polymer composition.

Acknowledgment. This work was funded by a European Community in the framework of the Marie Curie Early Stage Training Program POLY-MS (MEST-CT-2005-021029). J.S. acknowledges AkzoNobel for financial support. We thank Perry Derwig (ThermoFisher Scientific) for his contribution to our research with the Orbitrap experiments. Marco Koenraadt and Ber Yebio are acknowledged for the preparation of the acrylic resins. We acknowledge Dr. A. T. Jackson and Andreas Nasioudis for useful discussions.

Supporting Information Available: Tables giving a detailed comparison of the experimental data with the theoretical data for selected oligomers from PBA(C), the combinations of initiation and termination mechanisms of these series plus their

corresponding combined end group masses, and the intensities of the end groups and text giving the semiquantitative calculation on end group distribution. This material is available free of charge via the Internet at http://pubs.acs.org.

References and Notes

(1) Drin, A. P.; Efanova, V. V.; Shut, N. I. *J. Eng. Phys. Thermophys.* **1994**, *66*, 164–171.
(2) Okor, R. S. *J. Controlled Release* **1990**, *12*, 195–200.
(3) Chen, R. G.; Wu, S. H. Process for the preparation of crylic polymers for pharmaceutical coatings. US Patent 5,380,790, 1995.
(4) Capek, I.; Potisk, P. *Eur. Polym. J.* **1995**, *31*, 1269–1277.
(5) Matyjaszewski, K.; Xia, J. *Chem. Rev.* **2001**, *101*, 2921–2990.
(6) Buback, M.; Frauendorf, H.; Günzler, F.; Vana, P. *J. Polym. Sci., Part A: Polym. Chem.* **2007**, *45*, 2453–2467.
(7) van Herk, A. M. *Macromol. Rapid Commun.* **2001**, *22*, 687–689.
(8) Subrahmanyam, B.; Baruah, S. D.; Rahman, M.; Baruah, J. N.; Dass, N. N. *J. Polym. Sci., Part A: Polym. Chem.* **1992**, *30*, 2531–2549.
(9) Quan, C.; Soroush, M.; Grady, M. C.; Hansen, J. E.; Simonsick, W. J. *Macromolecules* **2005**, *38*, 7619–7628.
(10) Junkers, T.; Barner-Kowollik, C. *J. Polym. Sci., Part A: Polym. Chem.* **2008**, *46*, 7585–7605.
(11) Junkers, T.; Koo, S. P. S.; Davis, T. P.; Stenzel, M. H.; Barner-Kowollik, C. *Macromolecules* **2007**, *40*, 8906–8912.
(12) Pugh, C.; Fan, G.; Kasko, A. M. *Macromolecules* **2005**, *38*, 8071–8077.
(13) Jovanovic, R.; Dubé, M. A. *J. Appl. Polym. Sci.* **2001**, *82*, 2958–2977.
(14) Jovanovic, R.; Dubé, M. A. *J. Appl. Polym. Sci.* **2004**, *94*, 871–876.
(15) Mckenna, T. F.; Villanueva, A.; Santos, A. M. *J. Polym. Sci., Part A: Polym. Chem.* **1999**, *37*, 571–588.
(16) Hammond, J. M.; Hooper, J. F.; Stutchbury, J. E. *J. Polym. Sci., Polym. Symp.* **1975**, *49*, 117–125.
(17) Cheng, H. N.; Early, T. A. *Macromol. Symp.* **1994**, *86*, 1−14.
(18) Taniguchi, S.-i.; Takeshita, H.; Arimoto, M.; Miya, M.; Takenaka, K.; Shiomi, T. *Polymer* **2008**, *49*, 4889–4898.
(19) Whitehouse, C. M.; Dreyer, R. N.; Yamashita, M.; Fenn, J. B. *Anal. Chem.* **1985**, *57*, 675–679.
(20) Fenn, J. B.; Mann, M.; Meng, C. K.; Wong, S. F.; Whitehouse, C. M. *Science* **1989**, *246*, 64–71.
(21) Karas, M.; Bachmann, D.; Bahr, U.; Hillenkamp, F. *Int. J. Mass Spectrom. Ion Processes* **1987**, *78*, 53–68.
(22) Karas, M.; Hillenkamp, F. *Anal. Chem.* **1988**, *60*, 2299–2301.
(23) Nielen, M. W. F. *Mass Spectrom. Rev.* **1999**, *18*, 309–344.
(24) Peacock, P. M.; McEwen, C. N. *Anal. Chem.* **2004**, *76*, 3417–3428.
(25) Hanton, S. D. *Chem. Rev.* **2001**, *101*, 527–570.
(26) Scrivens, J. H.; Jackson, A. T. *Int. J. Mass Spectrom.* **2000**, *200*, 261–276.
(27) McEwen, C. N.; Peacock, P. M. *Anal. Chem.* **2002**, *74*, 2743–2748.
(28) van Rooij, G. J.; Duursma, M. C.; Heeren, R. M. A.; Boon, J. J.; de Koster, C. G. *J. Am. Soc. Mass Spectrom.* **1996**, *7*, 449–457.
(29) Kallos, G. J.; Tomalia, D. A.; Hedstrand, D. M.; Lewis, S.; Zhou, J. *Rapid Commun. Mass Spectrom.* **1991**, *5*, 383–386.
(30) Montaudo, G.; Montaudo, M. S.; Puglisi, C.; Samperi, F. *Macromolecules* **1995**, *28*, 4562–4569.
(31) Schriemer, D. C.; Li, L. *Anal. Chem.* **1997**, *69*, 4169–4175.
(32) Schriemer, D. C.; Li, L. *Anal. Chem.* **1997**, *69*, 4176–4183.
(33) Gruendling, T.; Guilhaus, M.; Barner-Kowollik, C. *Macromolecules* **2009**, *42*, 6366–6374.
(34) Craig, A. G.; Derrick, P. J. *J. Am. Chem. Soc.* **1985**, *107*, 6707–6708.
(35) Craig, A. G.; Derrick, P. J. *J. Chem. Soc., Chem. Commun.* **1985**, *13*, 891.
(36) Jackson, A. T.; Scrivens, J. H.; Williams, J. P.; Baker, E. S.; Gidden, J.; Bowers, M. T. *Int. J. Mass Spectrom.* **2004**, *238*, 287–297.
(37) Jackson, A. T.; Slade, S. E.; Scrivens, J. H. *Int. J. Mass Spectrom.* **2004**, *238*, 265–277.
(38) Jackson, A. T.; Slade, S. E.; Thalassinos, K.; Scrivens, J. H. *Anal. Bioanal. Chem.* **2008**, *392*, 643–650.
(39) Chen, R.; Li, L. *J. Am. Soc. Mass Spectrom.* **2001**, *12*, 832–839.
(40) Chen, R.; Yu, X.; Li, L. *J. Am. Soc. Mass Spectrom.* **2002**, *13*, 888–897.
(41) Arnould, M. A.; Wesdemiotis, C.; Geiger, R. J.; Park, M. E.; Buehner, R. W.; Vanderorst, D. *Prog. Org. Coat.* **2002**, *45*, 305–312.
(42) Wollyung, K. M.; Wesdemiotis, C.; Nagy, A.; Kennedy, J. P. *J. Polym. Sci., Part A: Polym. Chem.* **2005**, *43*, 946–958.
(43) Cerda, B. A.; Horn, D. M.; Breuker, K.; McLafferty, F. W. *J. Am. Chem. Soc.* **2002**, *124*, 9287–9291.
(44) Chaicharoen, K.; Polce, M.; Singh, A.; Pugh, C.; Wesdemiotis, C. *Anal. Bioanal. Chem.* **2008**, *392*, 595–607.
(45) Koo, S. P. S.; Junkers, T.; Barner-Kowollik, C. *Macromolecules* **2009**, *42*, 62–69.
(46) Koster, S.; Duursma, M. C.; Boon, J. J.; Heeren, R. M. A. *J. Am. Soc. Mass Spectrom.* **2000**, *11*, 536–543.
(47) Baker, E. S.; Gidden, J.; Anderson, S. E.; Haddad, T. S.; Bowers, M. T. *Nano Lett.* **2004**, *4*, 779–785.
(48) Trimpin, S.; Clemmer, D. E. *Anal. Chem.* **2008**, *80*, 9073–9083.
(49) Gidden, J.; Jackson, A. T.; Scrivens, J. H.; Bowers, M. T. *Int. J. Mass Spectrom.* **1999**, *188*, 121–130.